Dynamics of Protein Turnover, a Missing Dimension in Proteomics*

Julie M. Pratt‡, June Petty§, Isabel Riba-Garcia¶, Duncan H. L. Robertson‡, Simon J. Gaskell¶, Stephen G. Oliver§, and Robert J. Beynon‡‖

Functional genomic experiments frequently involve a comparison of the levels of gene expression between two or more genetic, developmental, or physiological states. Such comparisons can be carried out at either the RNA (transcriptome) or protein (proteome) level, but there is often a lack of congruence between parallel analyses using these two approaches. To fully interpret protein abundance data from proteomic experiments, it is necessary to understand the contributions made by the opposing processes of synthesis and degradation to the transition between the states compared. Thus, there is a need for reliable methods to determine the rates of turnover of individual proteins at amounts comparable to those obtained in proteomic experiments. Here, we show that stable isotope-labeled amino acids can be used to define the rate of breakdown of individual proteins by inspection of mass shifts in tryptic fragments. The approach has been applied to an analysis of abundant proteins in glucose-limited yeast cells grown in aerobic chemostat culture at steady state. The average rate of degradation of 50 proteins was 2.2%/h, although some proteins were turned over at imperceptible rates, and others had degradation rates of almost 10%/h. This range of values suggests that protein turnover is a significant missing dimension in proteomic experiments and needs to be considered when assessing protein abundance data and comparing it to the relative abundance of cognate mRNA species. ***Molecular & Cellular Proteomics 1:579–591, 2002.***

Four levels of analysis are commonly exploited in functional genomics: genome, transcriptome, proteome, and metabolome. The last three levels are all context-dependent; the complement of mRNA molecules, protein molecules, and metabolites all change with the physiological, developmental, or pathological state of living cells. A change in the proteome is probably the most important of these three for the analysis of gene action and interaction, but it is also the most difficult to study in a truly comprehensive manner (1).

"Classical" proteomics only compares amounts of proteins in cells in two different states or conditions; it does not address the dynamics of the proteome in the different biological states that are being compared nor does it provide information about the mechanisms whereby the system changes from one state to the other. The acquisition of a new steady-state level of any protein will be the outcome of the change in its rate of synthesis as compared with the change in its rate of degradation (2, 3). At the steady state, it is the balance between these two opposing processes that determines the concentration of any protein (4). To illustrate, an increase in the level of expression of a protein could be achieved by an enhanced rate of synthesis or a diminished rate of degradation. Despite its evident importance, the role of protein turnover has not previously been considered in analyses of the proteome. Yet the determination of the half-life of a large number of proteome components might do much to explain the marked disparity that is sometimes seen between transcriptome and proteome data (5–8). In addition, the requirements of one of the most energy-demanding processes in the cell, the aggregate process of protein synthesis and degradation, protein turnover, can be quantified on a protein-by-protein basis. In this article, we define an experimental strategy to analyze the dynamics of protein turnover, a missing dimension of proteomics.

EXPERIMENTAL PROCEDURES

Yeast Strain and Growth Conditions—The diploid yeast strain BY4743 (EUROSCARF accession number Y23935, www.uni-frankfurt.de/fb15/mikro/euroscarf/index.html) (9), a leucine auxotroph, was used throughout. Yeast were grown in glucose-limited chemostat culture as described previously (10) in a medium (Table I) containing 100 mg/liter DL-[$^2H_{10}$]leucine (98.5 atom % excess) at a dilution rate of 0.1 h^{-1}. After a minimum of seven doubling times, sufficient to ensure that cells were fully labeled, unlabeled L-leucine (1 g in 50 ml) was added, and the incoming medium was changed to one containing unlabeled L-leucine at 50 mg/liter. Sampling was at 0, 0.167, 0.667, 1, 2, 4, 6, 8, 10, 12, 24.5, and 51 h into the chase. This sampling frequency served to reduce the true dilution rate in the chase phase from a nominal 0.1 h^{-1} to an actual 0.086 h^{-1}. At each time point, cells were collected directly into ice-cold tubes containing cycloheximide (final concentration 100 μg/ml). Cells (40 ml at an A_{600} of ~1.6) were harvested and centrifuged at 5000 rpm for 5 min at 4 °C. The pellet was resuspended in 1 ml of ice-cold double distilled H_2O and transferred to a 1.5-ml microcentrifuge tube. Cells were repelleted by centrifugation at 10,000 rpm, the supernatant was dis-

From the ‡Department of Veterinary Preclinical Sciences, University of Liverpool, Crown Street, Liverpool L69 7ZJ, §School of Biological Sciences, 2.205 Stopford Building, University of Manchester, Oxford Road, Manchester M13 9PT, and ¶Michael Barber Centre for Mass Spectrometry, Department of Chemistry, University of Manchester Institute of Science and Technology, PO Box 88, Manchester M60 1QD, United Kingdom

Received, August 8, 2002, and in revised form, August 27, 2002

Published, MCP Papers in Press, August 28, 2002, DOI 10.1074/mcp.M200046-MCP200

TABLE I
Carbon-limited minimal medium for chemostat culture

Component	Final concentration
	g/liter
KH_2PO_4	2
$MgSO_4 \cdot 7H_2O$	0.55
NaCl	0.1
$CaCl_2 \cdot 2H_2O$	0.09
Glucose	2.5
NH_4SO_4	3.13
Uracil	0.02
Histidine	0.02
DL-Leucine[a]	0.1
Trace elements[b]	
$ZnSO_4 \cdot 7H_2O$	0.00007
$CuSO_4 \cdot 5H_2O$	0.00001
H_3BO_3	0.00001
KI	0.00001
$FeCl_3 \cdot 6H_2O$	0.00005
Vitamins	
Inositol	0.062
Thiamine/HCl	0.014
Pyridoxine	0.004
Calcium pantothenate	0.004
Biotin	0.0003

[a] DL-[$^2H_{10}$]Leucine was used in labeled media.

[b] Trace elements were made as two 10,000× stock solutions: solution 1, 10,000× $FeCl_3 \cdot 6H_2O$; solution 2, 10,000× $ZnSO_4 \cdot 7H_2O$, $CuSO_4 \cdot 5H_2O$, H_3BO, KI.

[c] Vitamins were made as a 600× stock solution and stored at −20 °C.

carded, and the yeast pellet was frozen in dry ice and stored at −80 °C. Cell pellets were thawed briefly on ice and resuspended in 300 μl of 20 mM HEPES, pH 7.5 containing one EDTA-free protease inhibitor mixture tablet/10 ml (Roche Diagnostics) and lysed by vortexing with glass beads (6 × 45 s with 45 s of cooling). DNase (6 μl of l mg/ml, Sigma) and RNase (2 μl of l mg/ml, Sigma) were added, and the lysate was held at 4 °C for 1 h. The lysate was centrifuged at 4000 rpm for 10 min at 4 °C, and the supernatant was assayed for protein (Coomassie plus protein assay, Pierce).

Protein Separation—Proteins (150 μg of soluble protein) from each of the 12 time points were then solubilized in 8 M urea, 2% (w/v) CHAPS, 20 mM dithiothreitol, and 0.5% 3–10 IPG Buffer (AP Biotech) for 1 h at 37 °C before centrifugation at 10,000 rpm for 10 min at 4 °C and application to 13-cm Immobiline pH 3–10 dry strips (AP Biotech) for in-gel rehydration (180 V-h at 30 V, 360 V-h at 60 V) and isoelectric focusing (500 V-h at 500 V, l000 V-h at 1000 V, and 16,000 V-h at 8000 V) using an IPGphor isoelectric focusing system (AP Biotech). Second-dimension analysis was by 12% (w/v) linear SDS-PAGE followed by Coomassie Blue staining. Gels were visually inspected, the same spot was excised from each gel, and peptides were obtained by in-gel reduction, alkylation with iodoacetamide, tryptic digestion, and extraction using a MassPrep™ digestion robot (Micromass, Manchester, UK).

Mass Spectrometry—Peptides were analyzed using a MALDI-TOF mass spectrometer (M@LDI™, Micromass, Manchester UK) covering the *m/z* range of 1000–4000 Th. Spectra were stacked above each other, and the peak differences between 0 h (heavy, fully labeled) and 51 h (light, fully unlabeled) were identified. Intermediate time points showed the gradual disappearance of peptides carrying heavy leucine and the gradual appearance of peptides carrying unlabeled leucine. Depending on the number of leucine residues in the peptide, the "heavy" and "light" peptides differed in mass by 9*n* Da, where *n* was the number of leucine residues in the peptide. The protein was identified by recording the masses of peptides in the 51-h spectrum (fully unlabeled) and including the leucine composition of each peptide (derived from comparison of the 0- and 51-h spectra) in a manual search of the yeast data base using MASCOT (www.matrixscience-.co.uk), which allows inclusion of composition data in its search (11).

Data Analysis—The monoisotopic peak intensities of the heavy and light tryptic peptides (A_H and A_L, respectively) were obtained and were used to calculate the relative isotope abundance at each time, *t* (RIA_t),[1] as the ratio:

$$RIA_t = \frac{A_H}{(A_L + A_H)} \quad \text{(Eq. 1)}$$

The value of RIA_t changes over time as the proteins, prelabeled with heavy leucine, are replaced by those labeled with light leucine. This is a consequence of two processes, namely loss of cells from the chemostat and loss through intracellular protein turnover. The generic form of the exponential equation relates the *RIA* at any time, *t*, to the values for *RIA* at $t = 0$ (RIA_0) and $t = \infty$ (RIA_∞, in practice, $t = 51$ h):

$$RIA_t = RIA_\infty + (RIA_0 - RIA_\infty)\ \exp(-k_{loss} \times t) \quad \text{(Eq. 2)}$$

Rather than use non-linear curve fitting to recover the values of three parameters (RIA_0, RIA_∞, and k_{loss}), RIA_0 was measured for 26 peptides derived from a total of 18 different proteins and yielded a value of 0.985 ± 0.001 (mean ± S.E., $n = 26$). The variance in this experimentally determined parameter was so low that it was fixed as the mean value in the non-linear curve fitting. Similarly, the value for RIA_∞ was set to zero since after 51 h, equivalent to seven doubling times, over 99% of the heavy labeled cells in the vessel at $t = 0$ h would have been lost from the vessel. By fixing these parameters, we also removed some of the error inherent in determination of the *RIA* at the start and end of the experiment where either the heavy or the light peak was small relative to the other and therefore the data were sometimes compromised by chemical noise in the mass spectrum. The fitted equation simplified to:

$$RIA_t = 0.985\ \exp(-k_{loss} \times t) \quad \text{(Eq. 3)}$$

The curve of this form was fitted to the (t, RIA_t) data using non-linear curve fitting to obtain k_{loss}, the error in the parameter estimate and the confidence limits for the fitted curve. In single time point experiments, k_{loss} was calculated from the value of RIA_t determined at a single time, *t*, according to the equation:

$$k_{loss} = -\ln(RIA_t/0.985)/t \quad \text{(Eq. 4)}$$

Finally, the true rate of degradation (k_{deg}) was calculated by simple subtraction of the constant dilution rate D from k_{loss} (the subtraction of a constant does not affect the error of the parameter estimate).

RESULTS

Determination of the rate of turnover of specific proteins is fraught with difficulty, and our strategy was designed to yield turnover rates under carefully controlled conditions. Our approach measures the kinetics of labeling of proteins with stable isotope-labeled amino acids and uses mass spectrometry to determine the presence of those labeled amino acids in tryptic peptides. In this respect it differs from other studies

[1] The abbreviations used are: *RIA*, relative isotope abundance; 2DGE, two-dimensional gel electrophoresis; CHAPS, 3-[(3-cholamidopropyl)dimethylammonio]-1-propanesulfonic acid; MALDI-TOF, matrix-assisted laser desorption ionization-time of flight.

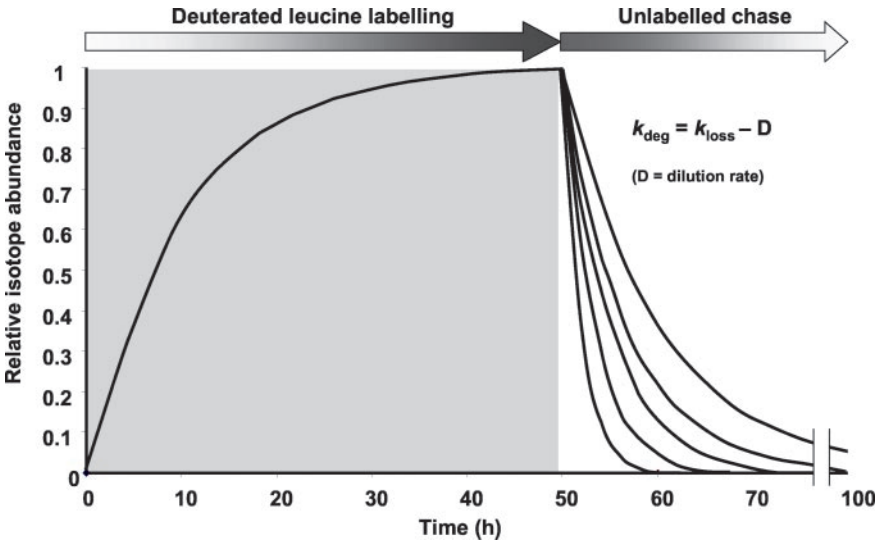

FIG. 1. **Overall strategy for determination of protein turnover rates.** Yeast cells were grown in chemostat culture in the presence of a stable isotope-labeled amino acid for which the cells are auxotrophic. After seven doubling times, over 99% of the amino acid in all proteins are labeled uniformly. Subsequently an excess of unlabeled amino acid is added instantaneously to the culture vessel, and the amino acid in the feedstock is also changed to the unlabeled form. This ensures that the isotope abundance precursor pool drops quickly and substantially. Subsequently newly synthesized proteins will contain unlabeled amino acid; the rate of replacement of labeled by unlabeled amino acid is defined by the rate of protein turnover. The lowest turnover rate that can be measured is equivalent to the dilution rate since that is the rate that cells (and therefore proteins) are leaving the culture vessel. The difference between the measured rate of loss of protein and the dilution rate is therefore the true intracellular degradation rate.

that have prelabeled proteins with stable isotope-labeled amino acids either to compare expression levels (12, 13), to determine the numbers of specific amino acids to aid in protein identification by peptide mass fingerprinting (11, 14–17), or to determine post-translational modifications (18). We measured the rate of turnover of several *Saccharomyces cerevisiae* proteins in glucose-limited aerobic continuous culture at the steady state. In continuous culture, the cells are maintained in a constant metabolic state, and the gain in biomass through growth is balanced by physical loss of cells as the cell suspension is displaced by incoming fresh medium. In this respect, continuous culture is superior to growth in "batch" culture in which nutrients are depleted, cell number increases, medium pH can fall, and the rate of growth declines.

The yeast cells were grown at a fixed dilution (doubling) rate, and proteins were uniformly labeled with a deuterated amino acid provided in the incoming growth medium. Subsequently a large excess of unlabeled amino acid was added instantaneously to the culture medium, and at the same time, the medium reservoir was switched to one containing the unlabeled amino acid. Because the cells are glucose-limited, the addition of an excess of the unlabeled amino acid does not affect the growth rate, but the labeled proteins are degraded and/or diluted into the daughter cells. The chosen precursor was decadeuterated leucine, labeled at all positions other than the α-amino and α-carboxyl groups and chosen because leucine is present in the great majority of tryptic peptides derived from the yeast proteome (11). Use of a leucine auxotrophic mutant of *S. cerevisiae* ensured that dilution of the label by endogenous leucine would be minimized. Finally, we have shown that the deuterium atom bonded to the α-carbon atom is metabolically labile (probably through transamination), and the relative incorporation of decadeuterated or nonadeuterated leucine provides a valuable insight into the metabolic lability of the precursor pool, important information in establishing the effectiveness of the labeling strategy (11, 14).

Proteins were prelabeled with heavy leucine for approximately 50 h, more than seven doubling times at a dilution rate of 0.1 h^{-1}. Thus, over 99% of the leucine in the cells would be the stable isotope-labeled form. Replacement of the entire leucine pool in this way had no effect on growth rate or on the overall pattern of proteins in a two-dimensional gel (results not shown). The chemostat was then injected with a large excess (20-fold) of unlabeled L-leucine to rapidly reduce the isotope abundance of the precursor pool. The feedstock was switched to unlabeled leucine, and samples of cells were taken from the culture vessel over the next 51 h. The unlabeled leucine pulse added to the growth vessel had no effect on CO_2 production, demonstrating that leucine was not being used as an alternative carbon source. Further, there were no quantitative differences in 2DGE patterns from cells before or after the chase with unlabeled leucine (results not shown). During the chase period, all newly synthesized proteins would only incorporate unlabeled leucine. The rate of loss of labeled protein (k_{loss}) is a composite term reflecting the sum of losses through dilution of the cells (synthesis *de novo*) or through degradation (Fig. 1).

At each sampling time before and throughout the chase period, cells were lysed, and proteins from the cleared lysate

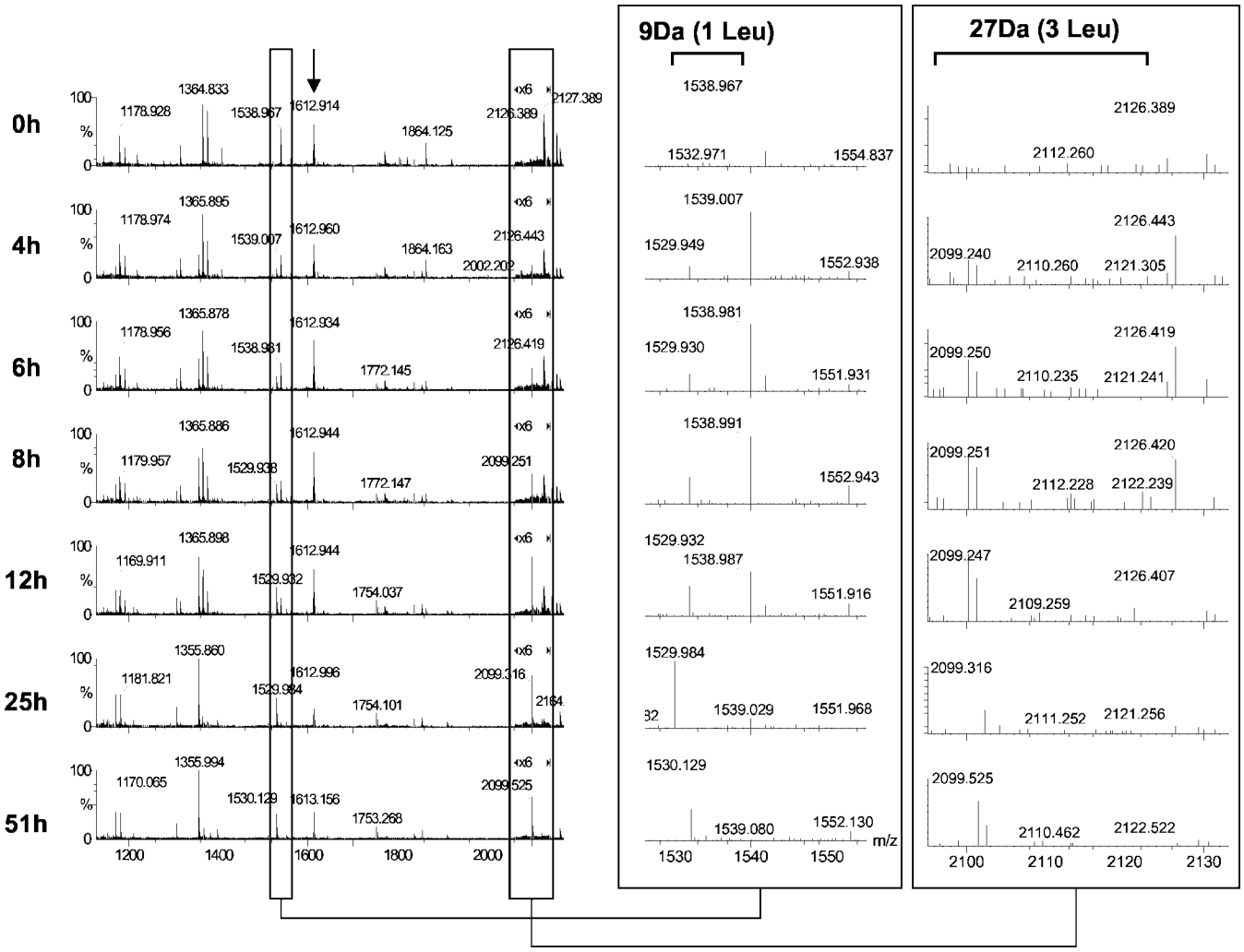

FIG. 2. **Changes in peptide mass fingerprint during unlabeled chase period.** Yeast cells, prelabeled in the presence of decadeuterated leucine, were subjected to a 51-h chase phase in the presence of excess unlabeled leucine. At different times, samples of the cell suspension were recovered, lysed, and resolved by 2DGE. Following staining with Coomassie Blue the same spot was recovered from each gel and subjected to in-gel tryptic digestion and MALDI-TOF mass spectrometry. The spectra on the *right* are amplified to show the behavior of single peptides (containing one and three leucine residues). The spectra on the *left* cover the *m/z* range from 1000 to 2500 Th. The *arrow* indicates a peptide that contains no leucine residues and therefore remains at the same mass throughout the chase.

were separated by 2DGE. The pattern of spots on the gels was very consistent (although this is not a prerequisite of the approach), and we could recover the same protein from each gel, which was then subjected to in-gel tryptic digestion followed by MALDI-TOF mass spectrometry (19). The profiles for individual peaks in the trypsin peptide mass fingerprint tracked the replacement of the labeled protein by the unlabeled protein as the cells continued to grow in culture. A representative set of MALDI-TOF data over 51 h, expanded to emphasize the behavior of individual peptides with one or multiple leucine residues, shows that the transition from fully labeled to fully unlabeled peptides was readily apparent (Fig. 2). Proteins were identified by peptide mass fingerprinting supplemented by the data on the leucine composition of each peptide derived from the separation between the heavy and light peaks (see "Experimental Procedures"). Incidentally, if the precursor pool had not been effectively "chased," peptides of intermediate masses, distributed binomially, would be expected (20). However, for peptides containing more than one leucine residue, the lack of peaks of mass values intermediate between the fully labeled and fully unlabeled forms is convincing proof that the relative isotope abundance of the precursor pool had been efficiently reduced to zero, a prerequisite of this approach. Of course, the lower limit on detection of these peptides of intermediate mass is influenced by the background noise in the spectrum. However, the lack of any such peaks above the noise floor is good evidence for an effective chase. The natural isotope abundance profiles of labeled peptides also confirmed that virtually all of the [$^2H_{10}$]leucine supplied in the medium was converted to

[$^2H_9$]leucine *in vivo* (probably through transamination).

The intensity of the monoisotopic peaks of the heavy and light tryptic fragments were measured for each sampling time point in the chase phase. The transition in intensity between the fully labeled and the fully unlabeled leucine-containing peptides is most simply defined by a single exponential curve that yields the first order rate constant for loss of the label from the protein (k_{loss}). To determine this rate constant, a single exponential curve was fitted to the set of RIA_t data for each leucine-containing tryptic peptide. Since multiple peptides in a single peptide mass fingerprint would be expected to contain leucine, each peptide should deliver an independent measure of the rate of turnover of the parent protein. For each protein, the first order rate constant was remarkably consistent whether derived from peptides with one or more than one leucine residue (Fig. 3). The errors in the fitted rate constants were typically less than 10% of the parameter value, and the concordance between the degradation rates, defined by multiple peptides derived from a single protein, was high. For all further analyses, we pooled the data from different peptides to yield a single fitted curve based on multiple determinations of RIA_t at each time point (Table II, spots 1–31).

Accurate measurement of the degradation rate of a single protein is of particular value in the elucidation of structural parameters that dictate intracellular stability. However, when applied to a global population of proteins in a proteome, multipoint determination of degradation rate would be extremely laborious. A higher throughput approach, more appropriate to global proteomic surveys, might be derived by analysis of a single time point during the chase period. For each protein, analysis of several (leucine-containing) peptides would still yield a statistical estimate of RIA_t at one value of t, which is related to an estimate of k_{loss} by the simple relationship $k_{loss} = -\ln(RIA_t/RIA_0)/t$.

We measured k_{loss} for several proteins recovered from 2DGE (Fig. 4 and Table II). For almost all proteins in this set, we were able to use data from multiple peptides containing between one and three leucine residues. For protein spots numbered 33 onward, the values of k_{loss} were recovered by sampling the cells at two time points (4 and 8 h), the degradation rates were calculated directly, and data from multiple peptides were combined to yield a statistical estimate of the certainty of the rate constant. For spots 1–31, the degradation rate constants had previously been assessed by non-linear curve fitting, and for a subgroup of these particular proteins, k_{loss} was redetermined using data for multiple peptides but at a single time point (Fig. 5, *panel A*). The correlation between the values of k_{loss} measured by the two methods was high ($r^2 = 0.87$, $n = 25$, $p < 0.001$). The single point method, whereby turnover rate is acquired from several peptides from the same protein, can yield as reliable an estimate as the more complex curve fitting approach. To test the reproducibility of the analytical method, we repeated the determination of turnover rate, from cell breakage onward, for a limited number of proteins ($n = 15$). Again, the correlation between the k_{loss} calculated in each experiment was very high ($r^2 = 0.86$, $p < 0.001$; Fig. 5, *panel B*).

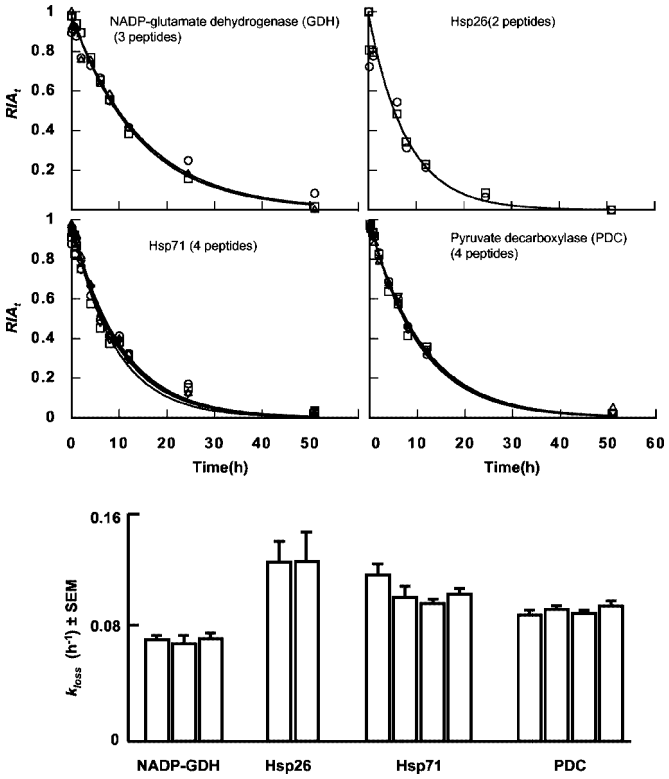

FIG. 3. **Determination of turnover rate by non-linear curve fitting.** For four representative protein spots taken from a series of two-dimensional gels, the peak intensities of the leucine-labeled and unlabeled peaks were measured by manual inspection of the mass spectra corresponding to a single tryptic peptide. For each peptide, the RIA_t of the labeled peptide was calculated and plotted against time. To determine the rate of turnover of the protein, a single exponential curve was fitted using non-linear curve fitting (FigP, Biosoft, Cambridge, UK). The different *symbols* indicate the RIA_t values determined for peptides derived from the same protein, and the *solid lines* are the best-fit curves for these different data sets. In most instances, the lines are so closely superimposable that the individual traces are not discernible. In the *lower panel*, the measured rates of loss of label are plotted for the individual peptides. Note that the true degradation rates must be corrected for the base-line rate of loss of protein from the chemostat at 0.086 h^{-1}.

Because the cells are in true steady state in the chemostat, the rate of loss of label includes irreversible losses by exit of cells from the system at a true rate of 0.086 h^{-1} (corrected for sampling). Thus, the intracellular degradation rates of the proteins should be corrected for this loss by simple subtraction of the dilution rate (Fig. 6). Of the ~50 proteins analyzed in this study, one-quarter are degraded at rates less than 0.01 h^{-1}. Two of these (spots 3 and 11, glutamate dehydrogenase and ketol-acid isomerase) are not significantly degraded at all and are only lost by dilution into daughter cells. At the other extreme, one protein (spot 41, methionine synthase) was de-

TABLE II

Rates of degradation of yeast proteins

Rates of degradation were measured for approximately 50 spots on a two-dimensional gel. For spots 1–31, gels were run under identical conditions for 12 time points. The same spots were then excized and analyzed for the *RIA* of heavy leucine in specific peptides; only data from good quality mass spectra are included. For each set of (RIA_t, t) data, non-linear curve fitting was used to acquire the first order rate constant for loss of label from the protein. This is a composite value representing the sum of the true intracellular degradation rate and the loss of protein due to exit of cells from the chemostat. Finally, the (RIA_t, t) data from all peptides were combined to generate a single, fitted value for the parameter estimate (all peptides). For spot 33 onward, only cells harvested at 4 and 8 h postchase were analyzed by the single point method. These estimates of the degradation rate were then aggregated into a single figure (last column). For each protein, the peptides are listed in decreasing order of abundance in the MALDI-TOF spectrum, and for each peptide, the number of leucine residues is given in square brackets. Peptides in addition to those used here for degradation analysis aided identification of the proteins. Spots 15 and 27 appear to contain more than a single protein, and spots 26, 27, and 28 would require further peptide analysis to determine their identity with confidence, although they still yield a valid degradation rate.

Spot no.	Protein ID	Peptide (observed $[M + H]^+$) [number of Leu residues]	Isotope removal (k_{loss}) (h^{-1}), curve fitting analysis ($k_{loss} \pm$ S.E. (n))	Isotope removal (k_{loss}), single point determination (mean $k_{loss} \pm$ S.E. (n))
1	Heat shock protein SSA1 (HS71)	1552.98 [2]	0.0972 ± 0.0028 (12)	
		2130.22 [2]	0.1035 ± 0.0040 (12)	
		1199.94 [2]	0.1117 ± 0.0081 (12)	
		1431.01 [1]	0.1012 ± 0.0078 (12)	
		All peptides	0.1032 ± 0.0051 (48)	
2	Pyruvate decarboxylase	1997.98 [1]	0.0901 ± 0.0021 (10)	
		1597.01 [1]	0.0930 ± 0.0029 (10)	
		1689.90 [1]	0.0897 ± 0.0035 (10)	
		All peptides	0.0919 ± 0.0024 (30)	0.0976 ± 0.0062 (10)
3	NADP-specific glutamate dehydrogenase	1188.80 [1]	0.0717 ± 0.0024 (10)	
		1605.14 [1]	0.0688 ± 0.0059 (10)	
		1468.86 [1]	0.0721 ± 0.0041 (10)	
		All peptides	0.0709 ± 0.0025 (30)	0.0633 ± 0.0024 (6)
4	Heat shock protein SSA1 or -2 (HS71/72) (fragment)	1552.98 [1]	0.1033 ± 0.0034 (12)	
		1675.90 [1]	0.1100 ± 0.0076 (12)	
		1431.03 [1]	0.1074 ± 0.0057 (12)	
		1816.07 [2]	0.1167 ± 0.0083 (11)	
		All peptides	0.1092 ± 0.0049 (47)	0.1221 ± 0.0033 (10)
5	Enolase II	1876.14 [1]	0.0865 ± 0.0038 (12)	
		1431.03 [2]	0.0906 ± 0.0069 (12)	
		2741.17 [2]	0.0909 ± 0.0023 (12)	
		All peptides	0.0893 ± 0.0041 (36)	0.0851 ± 0.0019 (10)
6	Enolase I pI ~7.5	1876.11 [1]	0.0933 ± 0.0027 (12)	
		1856.98 [1]	0.0993 ± 0.0103 (12)	
		2441.11 [2]	0.1048 ± 0.0075 (11)	
		All peptides	0.0950 ± 0.0058 (35)	
7	Enolase I pI ~7.7	1822.08 [2]	0.1130 ± 0.0077 (11)	
		2441.47 [2]	0.0987 ± 0.0024 (11)	
		1578.98 [2]	0.1190 ± 0.0128 (11)	
		1373.87 [1]	0.0998 ± 0.0025 (11)	
		All peptides	0.1034 ± 0.0029 (44)	0.0952 ± 0.0036 (10)
8	Phosphoglycerate kinase	1440.00 [3]	0.1145 ± 0.0025 (11)	
		1768.14 [3]	0.1079 ± 0.0026 (11)	
		1668.04 [2]	0.1058 ± 0.0025 (11)	
		2327.27 [1]	0.1005 ± 0.0042 (11)	
		2039.14 [2]	0.1005 ± 0.0051 (11)	
		All peptides	0.1058 ± 0.0027 (55)	0.1085 ± 0.0045 (10)
9	Yol 154wp	1617.94 [2]	0.1273 ± 0.0050 (12)	
		1961.58 [1]	0.1155 ± 0.0111 (11)	
		1228.75 [1]	0.1202 ± 0.0027 (10)	
		All peptides	0.1224 ± 0.0048 (33)	0.1241 ± 0.0026 (8)
10	Fructose-bisphosphate aldolase	2160.21 [1]	0.1209 ± 0.0073 (12)	
		1794.99 [1]	0.1157 ± 0.0053 (12)	
		1863.04 [1]	0.1273 ± 0.0069 (12)	
		2035.05 [1]	0.1178 ± 0.0039 (12)	
		All peptides	0.1203 ± 0.0054 (48)	0.1270 ± 0.0035 (8)

TABLE II—*continued*

Spot no.	Protein ID	Peptide (observed $[M + H]^+$) [number of Leu residues]	Isotope removal (k_{loss}) (h^{-1}), curve fitting analysis ($k_{loss} \pm$ S.E. (n))	Isotope removal (k_{loss}), single point determination (mean $k_{loss} \pm$ S.E. (n))
11	Ketol-acid isomerase	1355.99 [1]	0.0760 ± 0.0019 (11)	
		1170.06 [1]	0.0790 ± 0.0039 (12)	
		1181.94 [1]	0.0834 ± 0.0068 (12)	
		1306.09 [1]	0.0781 ± 0.0024 (11)	
		1530.13 [1]	0.0772 ± 0.0020 (11)	
		1753.27 [2]	0.0857 ± 0.0041 (11)	
		2099.52 [3]	0.0902 ± 0.0068 (11)	
		2145.45 [1]	0.0801 ± 0.0057 (11)	
		All peptides	0.0805 ± 0.0033 (90)	0.0680 ± 0.0021 (14)
12	Enolase I fragment	1159.82 [1]	0.1091 ± 0.0174 (9)	
		1856.97 [1]	0.1029 ± 0.0036 (10)	
		1578.91 [2]	0.1149 ± 0.0128 (9)	
		1373.78 [1]	0.1053 ± 0.0077 (9)	
		1756.03 [1]	0.1084 ± 0.0056 (9)	
		All peptides	0.1075 ± 0.0042 (37)	
13	Phosphoglycerate kinase fragment	1440.01 [3]	0.1113 ± 0.0035 (9)	
		1668.06 [2]	0.1034 ± 0.0037 (9)	
		All peptides	0.1073 ± 0.0034 (18)	
14	Glyceraldehyde-3-phosphate dehydrogenase 3	1752.78 [1]	0.0891 ± 0.0021 (8)	
		2591.20 [2]	0.0938 ± 0.0078 (9)	
		All peptides	0.0908 ± 0.0045 (17)	
15	Enolase I fragment	1856.96 [1]	0.1003 ± 0.0063 (12)	
		1578.89 [2]	0.1164 ± 0.0150 (11)	
		1373.78 [1]	0.1061 ± 0.0112 (11)	
		All peptides	0.1071 ± 0.0100 (34)	
15	Glyceraldehyde-3-phosphatase dehydrogenase 2	1752.87 [1]	0.0987 ± 0.0028 (12)	
16	Malate dehydrogenase	1395.92 [1]	0.1108 ± 0.0030 (11)	
		1350.03 [2]	0.1227 ± 0.0039 (11)	
		1592.96 [1]	0.0923 ± 0.0086 (10)	
		1332.90 [1]	0.1115 ± 0.0058 (10)	
		1638.01 [1]	0.1062 ± 0.0086 (11)	
		All peptides	0.1087 ± 0.0043 (53)	0.1077 ± 0.0166 (8)
17	Glyceraldehyde-3-phosphate dehydrogenase 3	1749.49 [1]	0.0945 ± 0.0017 (7)	
18	Glyceraldehyde-3-phosphate dehydrogenase 3	1750.67 [1]	0.0933 ± 0.0013 (9)	
19	Heat shock protein 26	1806.21 [1]	0.1262 ± 0.0150 (7)	
		2040.57 [2]	0.1265 ± 0.0228 (7)	
		All peptides	0.1263 ± 0.0187 (14)	0.1260 ± 0.0083 (6)
20	Fructose-bisphosphate aldolase	2390.20 [1]	0.0998 ± 0.0085 (6)	
		1863.07 [1]	0.0958 ± 0.0066 (6)	
		2035.13 [1]	0.0936 ± 0.0024 (6)	
		All peptides	0.0964 ± 0.0044 (18)	
21	Adenylate kinase	1456.01 [2]	0.1146 ± 0.0021 (7)	
		1994.30 [2]	0.1166 ± 0.0080 (8)	
		All peptides	0.1152 ± 0.0055 (15)	0.1299 ± 0.0139 (10)
22	Triosephosphate isomerase	1096.83 [1]	0.1019 ± 0.0017 (12)	
		1252.86 [1]	0.0932 ± 0.0042 (12)	
		2763.38 [2]	0.0954 ± 0.0038 (8)	
		All peptides	0.0966 ± 0.0019 (32)	0.1035 ± 0.0039 (10)
23	Glyceraldehyde-3-phosphate dehydrogenase 3 fragment	1753.06 [1]	0.0928 ± 0.0038 (10)	0.1046 ± 0.0066 (3)
25	Glyceraldehyde-3-phosphate dehydrogenase 3 fragment	1820.08 [2]	0.0991 ± 0.0043 (10)	
26	No ID	1752.47 [1]	0.1055 ± 0.0084 (6)	
27	Glyceraldehyde-3-phosphate dehydrogenase 2 fragment	1752.94 [1]	0.1046 ± 0.0067 (11)	
27	No ID	1785.86 [2]	0.1098 ± 0.0090 (5)	
28	No ID	1737.86 [2]	0.1130 ± 0.0550 (5)	
29	Cpn10	1591.96 [1]	0.1087 ± 0.0078 (7)	

TABLE II—*continued*

Spot no.	Protein ID	Peptide (observed $[M + H]^+$) [number of Leu residues]	Isotope removal (k_{loss}) (h^{-1}), curve fitting analysis ($k_{loss} \pm$ S.E. (n))	Isotope removal (k_{loss}), single point determination (mean $k_{loss} \pm$ S.E. (n))
		1525.93 [2]	0.1112 ± 0.0078 (7)	
		All peptides	0.0978 ± 0.0110 (14)	
30	Peptidylprolyl cis-trans isomerase	2098.05 [1]	0.1155 ± 0.0112 (7)	0.089 (1)
31	Heat shock protein 12	1437.80 [1]	0.1126 ± 0.0076 (7)	
		1745.84 [1]	0.1094 ± 0.0092 (8)	
		All peptides	0.1111 ± 0.0080 (15)	0.1037 ± 0.0222 (4)

Spot no.	Protein ID	Peptide (observed $[M + H]^+$)	Degradation rate (h^{-1}), single point (4 h, 8 h)	Degradation rate (h^{-1}), single point determination, all peptides (mean ± S.E. (n))
33	Microsomal protein of CDC48/PAS1/SEC18 family of ATPases	1756.11 [3]	0.1612, 0.1462	
		1246.84 [2]	0.1276, 0.1457	
		1578.04 [2]	0.1274, 0.1229	
		All peptides		0.1385 ± 0.0061 (6)
34	Actin binding protein; Abp1p	1583.22 [1]	0.0859, 0.0921	
		2133.39 [1]	0.0730, 0.0907	
		2662.76 [1]	0.0719, 0.0936	
		1715.25 [1]	0.1161, 0.1074	
		3035.64 [1]	0.0855, 0.1027	
		All peptides		0.0902 ± 0.0035 (10)
35	Kar 2p	1199.88 [2]	0.0773, 0.08187	
		1197.87 [1]	0.0985, 0.0805	
		1316.99 [2]	0.1046, 0.0894	
		1346.01 [1]	0.0877, 0.0771	
		1555.17 [2]	0.1176, 0.0909	
		1952.36 [3]	0.1437, 0.1039	
		1244.83 [1]	0.1007, 0.0838	
		1646.23 [1]	0.0771, 0.0973	
		All peptides		0.0945 ± 0.0058 (16)
36	Chain A proteinase A or vacuolar proteinase A Pep 4p	1700.05 [1]	0.1036, 0.1193	
		1212.85 [1]	0.0890, 0.0972	
		1571.98 [1]	0.1013, 0.1415	
		1889.17 [2]	0.0874, 0.1045	
		1916.12 [1]	0.1181, 0.1379	
		All peptides		0.1100 ± 0.0006 (10)
37	Sse1p; HSP70 family (homologous to Ssa1p and Sse2p)	1377.88 [1]	0.1216, 0.1253	
		1543.02 [2]	0.1515, 0.1169	
		1836.14 [1]	0.1267, 0.0998	
		1513.99 [1]	0.1182, 0.1181	
		1744.08 [2]	0.1411, 0.1211	
		1471.88 [1]	0.1128, 0.1163	
		1270.81 [1]	0.1077, 0.1271	
		All peptides		0.1217 ± 0.0020 (14)
38	Nuclear encoded mitochondrial protein; member of HSP70 family, most similar to *Escherichia coli* DnaK	1537.94 [1]	0.0943, 0.1036	
		1688.13 [1]	0.1118, 0.1150	
		1509.06 [2]	0.1024, 0.0918	
		1317.89 [2]	0.1642, 0.1656	
		All peptides		0.1186 ± 0.0123 (8)
39	YDL184w-b	1307.90 [1]	0.1083, 0.1009	
		1647.98 [1]	0.1040, 0.1018	
		1521.97 [1]	0.0901, 0.0913	
		1865.17 [1]	0.0815, 0.1135	

TABLE II—*continued*

Spot no.	Protein ID	Peptide (observed $[M + H]^+$)	Degradation rate (h^{-1}), single point (4 h, 8 h)	Degradation rate (h^{-1}), single point determination, all peptides (mean ± S.E. (*n*))
		All peptides		0.0989 ± 0.0026 (8)
40	Ssb2p; stress-seventy subfamily B/Ssb1p; stress-seventy subfamily B, involved in translation	1459.95 [1]	0.1123, 0.1163	
		1394.86 [2]	0.1364, 0.1288	
		1185.79 [1]	0.1545, 0.1348	
		1242.76 [2]	0.1567, 0.1002	
		1730.07 [1]	0.0917, 0.1347	
		2071.14 [1]	0.1145	
		All peptides		0.1255 ± 0.0062 (11)
41	Methionine synthase	1710.14 [1]	0.2059, 0.1525	
		1517.83 [1]	0.1859, 0.1633	
		All peptides		0.1769 ± 0.0119 (4)
42	Tkl1p; transketolase 1/yeast transketolase	1230.81 [2]	0.1331, 0.1172	
		1094.74 [1]	0.1105, 0.1016	
		1485.93 [2]	0.1209, 0.1206	
		1708.10 [1]	0.1372, 0.1004	
		1869.00 [1]	0.1092, 0.1023	
		2315.33 [1]	0.1107, 0.1004	
		All peptides		0.1137 ± 0.0034 (10)
43	Acetyl-CoA deacylase, mannose-containing glycoprotein that binds concanavalin A; Ach1p	1259.89 [1]	0.0996, 0.1111	
		1608.03 [1]	0.0996, 0.1122	
		1409.00 [1]	0.1132, 0.1059	
		1424.94 [1]	0.1082, 0.0977	
		1769.12 [1]	0.0754, 0.1145	
		All peptides		0.1037 ± 0.0020 (10)
44	Pyruvate kinase Cdc19p; required for start of cell cycle	1501.98 [1]	0.0876, 0.0879	
		1315.89 [1]	0.0973, 0.0959	
		1227.75 [2]	0.0981, 0.1041	
		2001.22 [3]	0.0867, 0.1024	
		1761.03 [1]	0.0893, 0.0781	
		All peptides		0.0927 ± 0.0020 (10)
45	Lipoamide dehydrogenase, chain A, FAD flavoprotein	1174.67 [1]	0.1147, 0.1102	
		1564.48 [1]	0.1115, 0.1172	
		1496.43 [1]	0.1284, 0.1094	
		1801.00 [1]	0.1077, 0.1145	
		All peptides		0.1142 ± 0.0025 (8)
46	ATPase1 α su	1553.84 [1]	0.1037, 0.1160	
		1325.80 [2]	0.1166, 0.1267	
		1350.83 [1]	0.1103, 0.1114	
		1458.84 [1]	0.1016, 0.1108	
		1438.93 [1]	0.1077, 0.1150	
		1273.75 [2]	0.1032, 0.1176	
		1602.91 [1]	0.1155, 0.1131	
		1935.08 [1]	0.1037, 0.1153	
		All peptides		0.1117 ± 0.0020 (16)
47	Shm2p serine hydroxymethyltransferase	1196.70 [1]	0.1607, 0.1305	
		1168.69 [1]	0.1471, 0.1126	
		1572.99 [1]	0.1646, 0.1318	
		1728.05 [3]	0.1305, 0.1163	
		1690.00 [1]	0.1545, 0.1147	
		1707.02 [1]	0.1501	
		All peptides		0.1376 ± 0.0060 (11)
48	G4p1 ± Arc1p; associated with tRNA and aminoacyl-tRNA synthetases	1259.64 [1]	0.1049, 0.1067	

TABLE II—*continued*

Spot no.	Protein ID	Peptide (observed $[M + H]^+$)	Degradation rate (h^{-1}), single point (4 h, 8 h)	Degradation rate (h^{-1}), single point determination, all peptides (mean ± S.E. (*n*))
		1243.64 [1]	0.1155, 0.1082	
		1706.61 [1]	0.0929, 0.1048	
		1574.52 [1]	0.0936, 0.0952	
		1690.63 [1]	0.0907, 0.1128	
		All peptides		0.1025 ± 0.0026 (10)
49	Idh2p NAD^+-dependent isocitrate dehydrogenase	1435.73 [2]	0.1113, 0.1241	
		1448.78 [1]	0.1017, 0.0991	
		1320.74 [1]	0.1024, 0.1035	
		All peptides		0.1070 ± 0.0038 (6)
50	Tpm1p; tropomyosin I	1644.89 [1]	0.1013, 0.1440	
		1800.99 [1]	0.1230, 0.1411	
		1958.02 [1]	0.0965, 0.1418	
		2039.06 [2]	0.1186	
		All peptides		0.1246 ± 0.0087 (7)
51	Bmh2p; brain modulosignalin homologue/protein from family 14.3.3	1215.59 [1]	0.0954, 0.1042	
		1110.62 [1]	0.1000, 0.1066	
		1834.04 [1]	0.0992, 0.1028	
		1461.79 [1]	0.1090, 0.1016	
		1367.77 [1]	0.1187, 0.1048	
		2001.93 [1]	0.1093, 0.1039	
		1969.90 [1]	0.1277, 0.0894	
		1985.98 [1]	0.1450, 0.1010	
		All peptides		0.1074 ± 0.0020 (16)
52	Brain modulosignalin homologue or BMHI	1834.04 [1]	0.1008, 0.1043	
		1491.78 [1]	0.1015, 0.1119	
		1215.39 [1]	0.1037, 0.0953	
		All peptides		0.1029 ± 0.0022 (6)

graded intracellularly at a rate of over 9%/h. Even allowing the caveat that we selected high abundance proteins, the range of degradation rates is over 9-fold in cells that are in balanced exponential growth.

DISCUSSION

We deliberately focused on the more abundant proteins to develop the approach and to assess the dynamics of bulk proteins in exponentially growing cells. Although such abundant proteins might be expected to be long-lived, the degradation rates are remarkably heterogeneous, which raises important issues of selectivity of degradation of this class of proteins. For example, a simple process of vacuolar internalization cannot impose any heterogeneity on degradation rates, and whatever the mechanism of intracellular proteolysis, selective mechanisms must operate. A previous study of selected yeast proteins (including several analyzed here) implied that they were not degraded in exponential growth (21), but the labeling/chase time periods were short, which serves to emphasize the importance of the extended labeling/chase protocol in accessing lower turnover rates. Moreover, the radiolabeling approach used previously (21, 22) cannot readily be combined with the identification step, and autoradiography of the entire protein spot means that the enhanced statistical certainty deriving from multiple peptides is inaccessible.

The ability to determine, with a high degree of accuracy and precision, the rate of degradation of individual proteins opens up an additional dimension in proteomics. The "single point" method yields a reliable parameter estimate and a statistical certainty of high quality and would be particularly suited to studies of relative rates of protein degradation. For more detailed analyses of the routes and rates of degradation of individual proteins, serial sampling and multiple time point determination of isotope abundance creates a data set that is amenable to non-linear curve fitting. The labeling strategy used here works optimally when cells are maintained in steady-state culture, but there will be other labeling protocols that are more amenable to batch culture, organ culture, or intact animals. It would, for example, be feasible to measure the rate of synthesis of each protein by transient exposure to the precursor label, although this would require knowledge of the precursor isotope abundance, and unlike radioisotope labeling, the degree of incorporation of the stable isotope label has to be substantial (>20%) for reliable estimation of the abundance of mass shifted peptides.

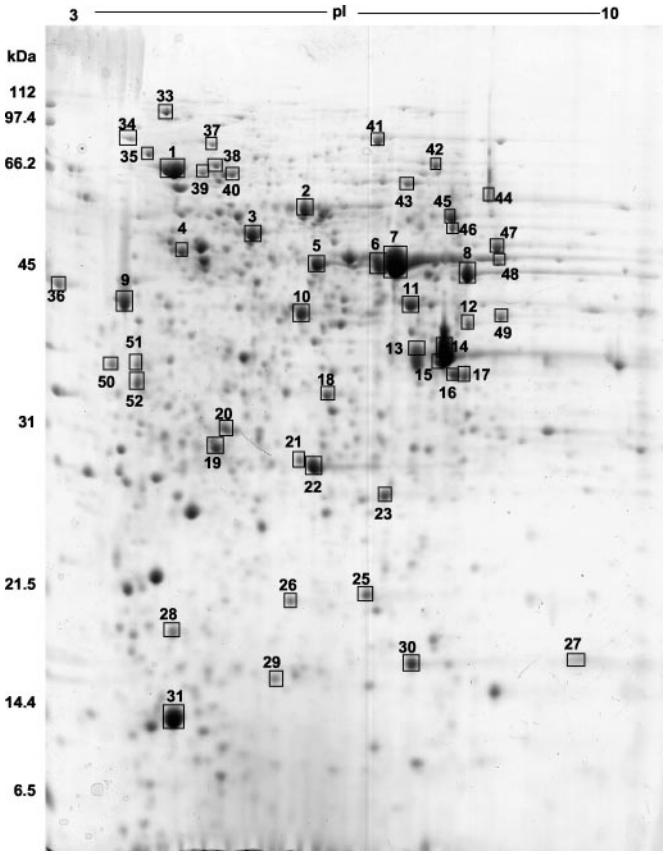

FIG. 4. **Measurement of the turnover rate of yeast proteins.** Yeast proteins were separated by 2DGE (first dimension pI 3–10, second dimension 12% linear gel) and stained with Coomassie Blue. Selected, high abundance spots were recovered from gels corresponding to multiple time points (between 10 and 12, curve fitting approach, one or two time points for single point determinations), and the rate of degradation was determined as described in the text. The positions of specific proteins are indicated on the gel, and the rates of degradation are presented in Table II. Spots 28 and 32 were not analyzable and have been omitted from Table II. Spots 15 and 27 contained peptides from more than one protein.

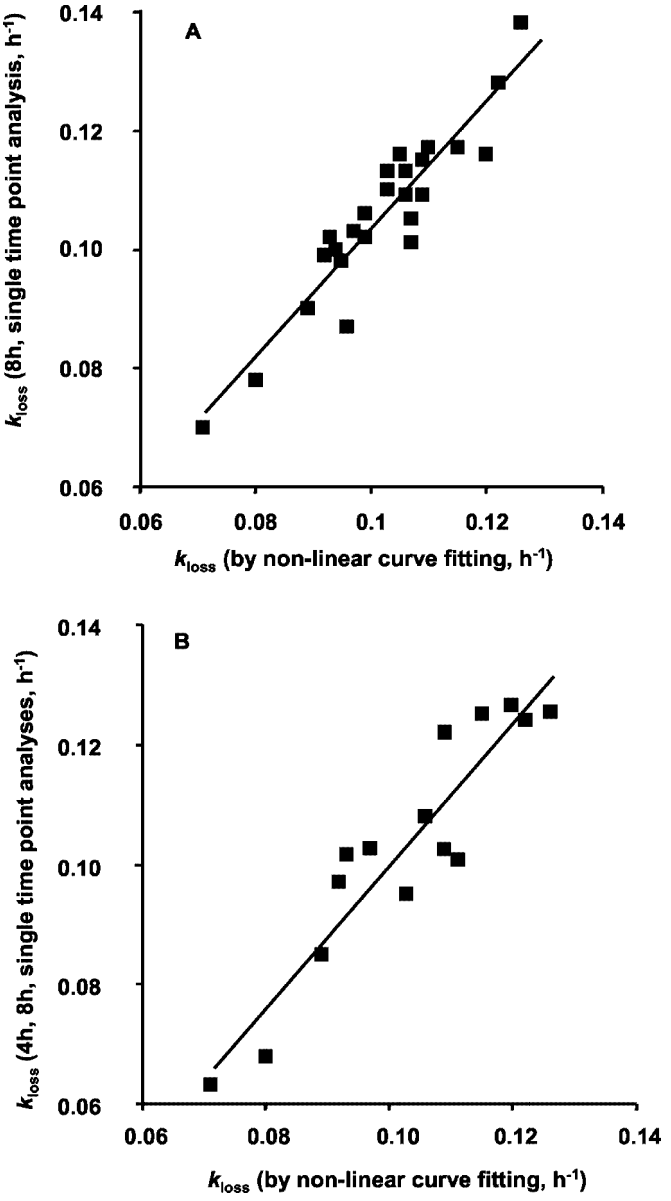

FIG. 5. **Correlation between curve fitting and single point analysis.** *Panel A*, for 25 proteins, the value of k_{loss} determined by nonlinear curve fitting was plotted against the value obtained from single point analysis using multiple peptides in the MALDI-TOF spectrum but at a single time point of 8 h. *Panel B*, to assess the reproducibility of the analysis, for a subset of the proteins ($n = 15$) we repeated the determination of turnover rate, from cell breakage onward, using the single point method. For both plots, the regression line is superimposed on the data.

The method, in common with all other methods to measure protein turnover rates, is limited in the ability to define the rate of high turnover proteins. But high turnover proteins would be manifest by a very rapid loss of heavy label, and even if the precise rate of degradation was not quantifiable, the protein would still be classified as "high turnover." By the same arguments, the proteins for which the rate of loss of label is equal to dilution rate can be classified as "extremely low turnover," and two such proteins have been identified in this set. The mechanism whereby a protein evades the degradative machinery of the cell can cast as much light on the molecular recognition and enzymology of the process as can the study of high turnover proteins.

Although it is most simple to obtain multiple measures of turnover rate from the peptides derived from an excised spot, there is no reason why this method could not be applied to peptides isolated by liquid chromatography. A liquid chromatography/mass spectrometry experiment would yield RIA_t, but this would be as a single value. Further improvement in the statistical certainty of the measure would be obtained either from the use of multiple time points, to which the curve fitting approach could be applied, or by sufficiently exhaustive coverage of a liquid chromatography profile to recover turnover rates from multiple unique peptides deriving from one protein. In this respect, the choice of leucine is important as it is the

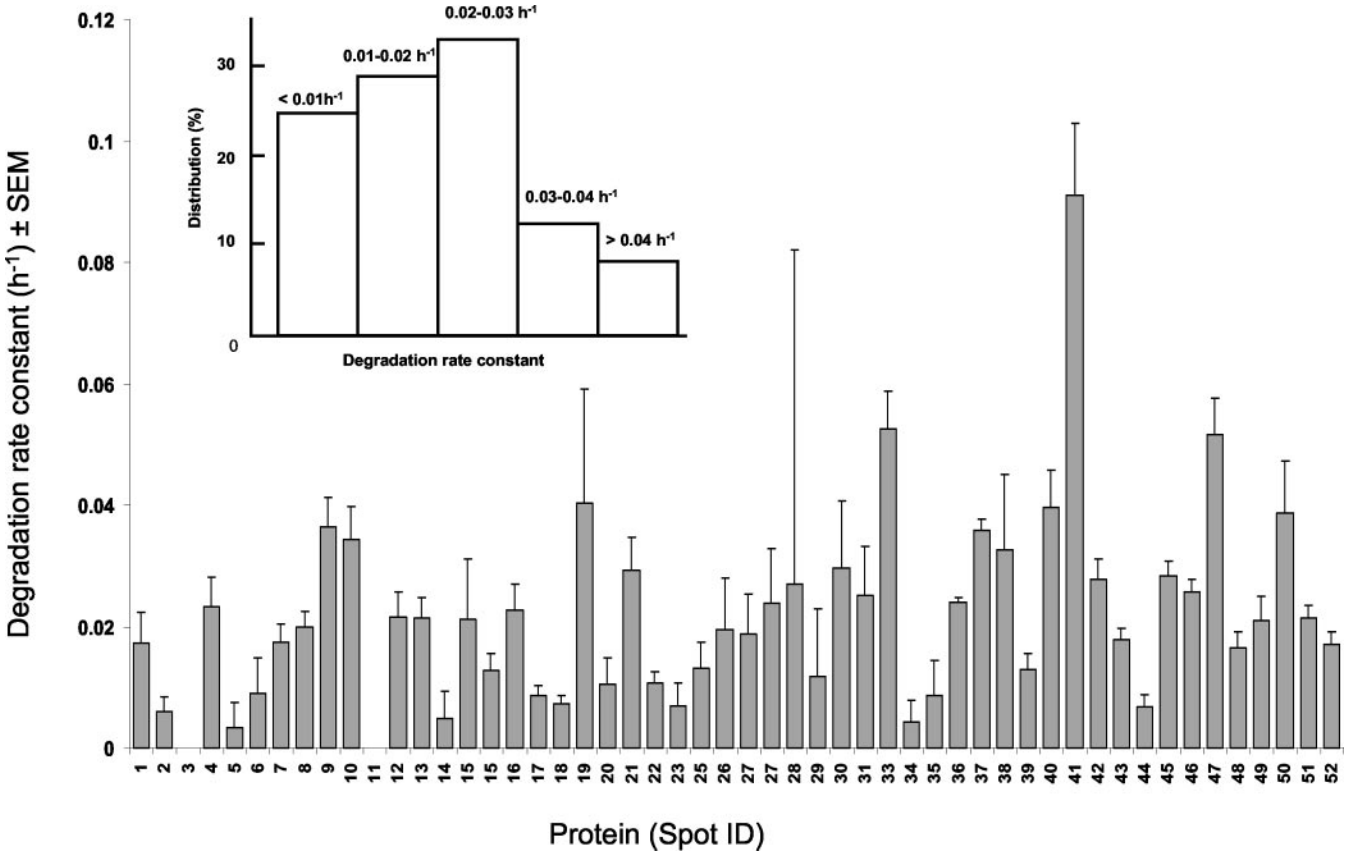

FIG. 6. **True degradation rates of soluble yeast proteins.** For each of the proteins indicated on the two-dimensional gel (Fig. 4), the true intracellular degradation rate was calculated by correction for the cell dilution rate. Data are presented with the error indicated (spots 1–31, S.E. for the fitted value of the parameter estimate, spots 33 onward, mean ± S.E. for multiple peptides). For values of *n*, see Table II. The *inset* shows a distribution profile of degradation rates for these ~50 relatively high abundance yeast proteins.

most abundant amino acid in the proteome (11).

We plan to extend this analysis to the study of proteins commonly occurring in supramolecular complexes, the assembly and conformation of which have profound effects on function and stability. In this study we measured the turnover rate of a protein species that migrates to a single spot. However these protein molecules could have been part of widely different functional complexes with other proteins, and the turnover rate could just be an average of a number of distinct rates that operate at the level of supramolecular complexes. Including a fractionation step that preserves protein-protein interactions prior to analysis would separate proteins that are involved in multiple tasks into different fractions. Subsequent analysis of turnover could reveal the same protein to exhibit a different turnover rate depending on the function of the complex from which it derived.

Despite the importance of protein degradation in maintenance of the proteome, the process remains largely elusive. The discovery of the ubiquitin conjugation and proteasome systems has identified the marking and proteolytic mechanisms that are responsible for degradation of many intracellular proteins (23, 24). The key area that is poorly understood is that of the selectivity of the process whereby different proteins are committed to degradation at dramatically different rates. The accurate determination of degradation rate is an essential parameter in the study of the regulation and manipulation of protein turnover, for instance in the industrial production of recombinant proteins. Further, the single peptide approach can provide a rapid overview of the range and scope of protein degradation for large numbers of constituents of the proteome. With the development of such approaches, the dynamics of the proteome need no longer be considered inaccessible, and the relationship between transcriptome and proteome should be better understood.

Acknowledgments—We are grateful to Sue Francis and Joanne Connolly for technical assistance.

* This work was supported by a grant from the Biotechnology and Biological Sciences Research Council (Project Grant 26/G13495 to R. J. B., S. J. G., and S. G. O.) and by the COGEME (Consortium for the Functional Genomics of Microbial Eukaryotes) program (to S. G. O., co-ordinator). The costs of publication of this article were defrayed in part by the payment of page charges. This article must therefore be hereby marked "*advertisement*" in accordance with 18 U.S.C. Section 1734 solely to indicate this fact.

‖ To whom correspondence should be addressed. Tel.: 44-151-794-4312; Fax: 44-151-794-4243; E-mail: r.beynon@liv.ac.uk.

REFERENCES

1. Miklos, G. L., and Maleszka, R. (2001) Protein functions and biological contexts. *Proteomics* **1,** 169–178
2. Gottesman, S., and Maurizi, M. R. (1992) Regulation by proteolysis: energy-dependent proteases and their targets. *Microbiol. Rev.* **56,** 592–621
3. Hochstrasser, M., Johnson, P. R., Arendt, C. S., Amerik, A., Swaminathan, S., Swanson, R., Li, S. J., Laney, J., Pals-Rylaarsdam, R., Nowak, J., and Connerly, P. L. (1999) The *Saccharomyces cerevisiae* ubiquitin-proteasome system. *Philos. Trans. R. Soc. Lond. B Biol. Sci.* **354,** 1513–1522
4. Benaroudj, N., Tarcsa, E., Cascio, P., and Goldberg, A. L. (2001) The unfolding of substrates and ubiquitin-independent protein degradation by proteasomes. *Biochimie* (*Paris*) **83,** 311–318
5. Gygi, S. P., Rochon, Y., Franza, B. R., and Aebersold, R. (1999) Correlation between protein and mRNA abundance in yeast. *Mol. Cell. Biol.* **19,** 1720–1730
6. Ideker, T., Thorsson, V., Ranish, J. A., Christmas, R., Buhler, J., Eng, J. K., Bumgarner, R., Goodlett, D. R., Aebersold, R., and Hood, L. (2001) Integrated genomic and proteomic analyses of a systematically perturbed metabolic network. *Science* **292,** 929–934
7. Griffin, T. J., Gygi, S. P., Ideker, T., Rist, B., Eng, J., Hood, L., and Aebersold, R. (2002) Complementary profiling of gene expression at the transcriptome and proteome levels in *Saccharomyces cerevisiae. Mol. Cell. Proteomics* **1,** 323–333
8. Chen, G., Gharib, T. G., Huang, C. C., Taylor, J. M., Misek, D. E., Kardia, S. L., Giordano, T. J., Iannettoni, M. D., Orringer, M. B., Hanash, S. M., and Beer, D. G. (2002) Discordant protein and mRNA expression in lung adenocarcinomas. *Mol. Cell. Proteomics* **1,** 304–313
9. Brachmann, C. B., Davies, A., Cost, G. J., Caputo, E., Li, J., Hieter, P., and Boeke, J. D. (1998) Designer deletion strains derived from *Saccharomyces cerevisiae* S288c: a useful set of strains and plasmids for PCR-mediated gene disruption and other applications. *Yeast* **14,** 115–132
10. Baganz, F., Hayes, A., Farquhar, R., Butler, P. R., Gardner, D. C., and Oliver, S. G. (1998) Quantitative analysis of yeast gene function using competition experiments in continuous culture. *Yeast* **14,** 1417–1427
11. Pratt, J. M., Robertson, D. H., Gaskell, S. J., Riba-Garcia, I., Hubbard, S. J., Sidhu, K., Oliver, S. G., Butler, P., Hayes, A., Petty, J., and Beynon, R. J. (2002) Stable isotope labelling in vivo as an aid to protein identification in peptide mass fingerprinting. *Proteomics* **2,** 157–163
12. Ong, S. E., Blagoev, B., Kratchmarova, I., Kristensen, D. B., Steen, H., Pandey, A., and Mann, M. (2002) Stable isotope labeling by amino acids in cell culture, SILAC as a simple and accurate approach to expression proteomics. *Mol. Cell. Proteomics* **1,** 376–386
13. Jiang, J., and English, A. M. (2002) Quantitative analysis of the yeast proteome by incorporation of isotopically labeled leucine. *J. Proteome Res.* **1,** 345–350
14. Hirayama, K., Yuji, R., Yamada, N., Noguchi, K., Yamaguchi, Y., Enokizono, J., Katao, K., Arata, Y., and Shimada, I. (1998) Convenient peptide mapping of immunoglobulin g2b and differentiation between leucine and isoleucine residues by mass spectrometry using 2h-labeled leucine. *J. Mass. Spectrom. Soc. Jpn.* **46,** 83–89
15. Chen, X., Smith, L. M., and Bradbury, E. M. (2000) Site-specific mass tagging with stable isotopes in proteins for accurate and efficient protein identification. *Anal. Chem.* **72,** 1134–1143
16. Hunter, T. C., Yang, L., Zhu, H., Majidi, V., Bradbury, E. M., and Chen, X. (2001) Peptide mass mapping constrained with stable isotope-tagged peptides for identification of protein mixtures. *Anal. Chem.* **73,** 4891–4902
17. Engen, J. R., Bradbury, E. M., and Chen, X. (2002) Using stable-isotope-labeled proteins for hydrogen exchange studies in complex mixtures. *Anal. Chem.* **74,** 1680–1686
18. Zhu, H., Hunter, T. C., Pan, S., Yau, P. M., Bradbury, E. M., and Chen, X. (2002) Residue-specific mass signatures for the efficient detection of protein modifications by mass spectrometry. *Anal. Chem.* **74,** 1687–1694
19. Shevchenko, A., Jensen, O. N., Podtelejnikov, A. V., Sagliocco, F., Wilm, M., Vorm, O., Mortensen, P., Boucherie, H., and Mann, M. (1996) Linking genome and proteome by mass spectrometry: large-scale identification of yeast proteins from two dimensional gels. *Proc. Natl. Acad. Sci. U. S. A.* **93,** 14440–14445
20. Papageorgopoulos, C., Caldwell, K., Shackleton, C., Schweingrubber, H., and Hellerstein, M. K. (1999) Measuring protein synthesis by mass isotopomer distribution analysis (MIDA). *Anal. Biochem.* **267,** 1–16
21. Futcher, B., Latter, G. I., Monardo, P., McLaughlin, C. S., and Garrels, J. I. (1999) A sampling of the yeast proteome. *Mol. Cell. Biol.* **19,** 7357–7368
22. Grünenfelder, B., Rummel, G., Vohradsky, J., Roder, D., Langen, H., and Jenal, U. (2001) Proteomic analysis of the bacterial cell cycle. *Proc. Natl. Acad. Sci. U. S. A.* **98,** 4681–4686
23. Varshavsky, A. (1996) The N-end rule: functions, mysteries, uses. *Proc. Natl. Acad. Sci. U. S. A.* **93,** 12142–12149
24. DeMartino, G. N., and Slaughter, C. A. (1999) The proteasome, a novel protease regulated by multiple mechanisms. *J. Biol. Chem.* **274,** 22123–22126